Multidisciplinary Optimization Group

OpenPulse - Open source code for numerical modelling of low-frequency acoustically induced vibration in gas pipeline systems

Theory Reference B: Structural vibration module
V1.0

Olavo M. Silva, Lucas V. Q. Kulakauskas, Jacson G. Vargas,
André Fernandes, José L. Souza, Ana Rocha and Diego M. Tuozzo
olavo.silva@mopt.com.br

21 May 2020

1 Introduction

In oil refinery plants, the structural vibration behavior of gas pipeline systems can be strongly affected by the response of the acoustic domain represented by the gas being transported through pressurized pipes, cylinders and other related components. The resultant Acoustically Induced Vibration (AIV) can be a cause of failure, for example, in reciprocating compression systems. In this work, the authors present a strategy based on the acoustic Transfer Matrix Method (see Theory Reference A) and on the Timoshenko beam theory to represent the referred acoustic-structure interaction in gas pipelines as a weakly coupled system, modeled by the Finite Element Method (FEM). The suggested procedure has several benefits for low frequency analysis such as:

- i) assuming propagation of acoustic plane waves, TMM-based procedures are more advantageous in terms of computational cost and accuracy than FEM for 1D acoustics even considering filters, volumes, valves and branches as equivalent impedances; in addition, the reflection effects of pipe elbows can be considered;
- ii) structural FEM models based on beam theory are well consolidated for predicting global vibrations of pipe systems; in this work, the C0 Timoshenko's formulation also allows to obtain better stress/strain values when compared to other classical formulations;

- iii) the one-way coupling is sufficient to represent the acoustic-structure interaction considering low excitation frequencies and typical relations between internal diameter and wall thickness of pipes used in refinery plants.

This text is based in the Section 5.4 of the book: *The Finite Element Method: Linear Static and Dynamic Finite Element Analysis* [4], originally published by Thomas J. R. Hughes in 1987. Some parts were taken directly from the referred book. Here, different from what is done by Hughes, it is considered linear elastodynamics by keeping the inertial forces in the "strong form" of the equilibrium equation.

The classical Euler-Bernoully beam theory requires C^1-continuity, resulting in schemes that can be complicated to be implemented for multidimensional problems. On the other hand, the classical Timoshenko beam theory requires only C^0-continuity, enabling the use of finite element shape functions that are easily constructed.

However, some analytical methodologies (based on "fixed" cubic polynomials to represent bending, which are basis for the analytical solution of the problem) used to implement some Timoshenko beam elements are not interesting in the sense of changing shape functions or in adopting methodologies to improve stress calculations. So, we choose the "original finite element technology" to implement our Timoshenko beam element.

2 Main assumptions

2.1 Domain

We assume from the start that the domain is divided into segments (or elements), interconnected at nodal points [4]:

$$\Omega = \bigcup_{e=1}^{nel} \Omega^e, \tag{1}$$

$$\Omega^e = \{(x_1^e, x_2^e, x_3^e) | x_1^e \in [0, h^e], (x_2^e, x_3^e) \in A^e \subset R^2\}. \tag{2}$$

We initially assume that the (x_1^e, x_2^e, x_3^e)-axes are *locally* defined with respect to the beam segment and are *principal axes* [4]. See Fig. 1. So,

$$\int_A x_2^e dA = \int_A x_3^e dA = \int_A x_2^e x_3^e dA = 0. \tag{3}$$

To save writing, the superscript e will be omitted in some expressions.

In *OpenPulse*, we also consider the possibility of applying an offset between local coordinates and the beam's neutral axis as described in [6]. For the sake of simplicity, this theory reference details the main hypotheses and physical meaning by considering only the assumption in Eq. (3)**.**

2.2 Shear stress

Different from Euler-Bernoulli theory, here σ_{21} $(= \sigma_{12})$ and σ_{31} $(= \sigma_{13})$ are not null $(\sigma_{\gamma 1} \neq 0)$. However, $\sigma_{23} = 0$ and $\sigma_{32} = 0$ (there is no bending along x_2 and x_3). So,

$$\sigma_{\beta\gamma} = 0 \tag{4}$$

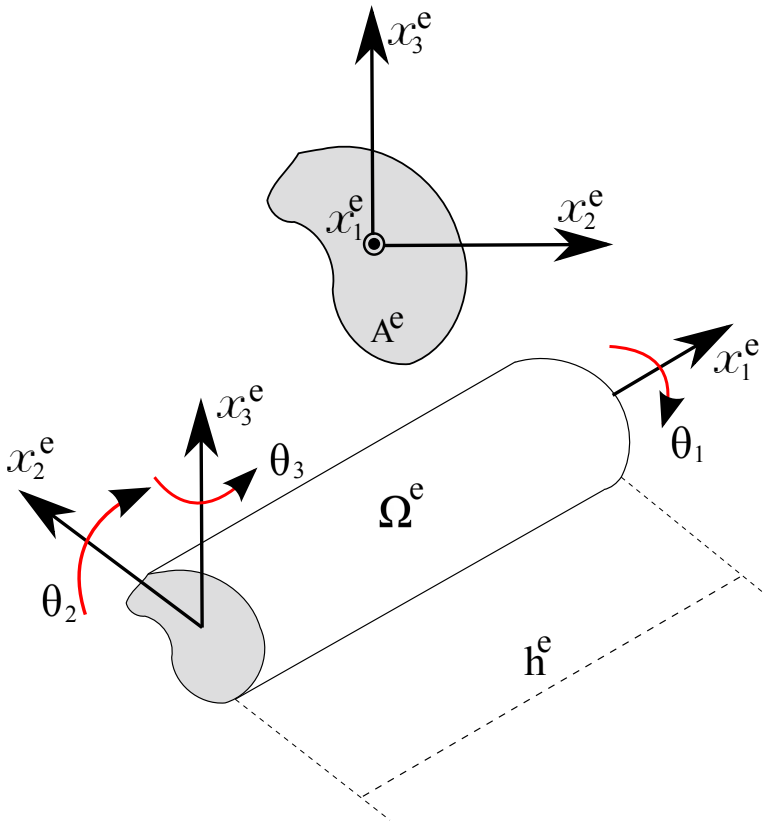

Figure 1: Local coordinates [Source: author].

2.3 Kinematic constraints

The tridimensional displacements of a point (x_1, x_2, x_3) that belongs to a cross-sectional area A placed in x_1 are given by [1, 4, 7]:

$$u_1(x_1, x_2, x_3, t) = w_1(x_1, t) - x_2\theta_3(x_1, t) + x_3\theta_2(x_1, t), \tag{5}$$

$$u_2(x_1, x_2, x_3, t) = w_2(x_1, t) - x_3\theta_1(x_1, t), \tag{6}$$

$$u_3(x_1, x_2, x_3, t) = w_3(x_1, t) + x_2\theta_1(x_1, t). \tag{7}$$

Consequently, the movement of a given point (x_1, x_2, x_3) in Ω^e is described by:

$$\boldsymbol{u}(x_1, x_2, x_3, t) = \begin{Bmatrix} u_1(x_1, x_2, x_3, t) \\ u_2(x_1, x_2, x_3, t) \\ u_3(x_1, x_2, x_3, t) \end{Bmatrix}. \tag{8}$$

The translation components w_i of the neutral line and the rotation angles θ_i of the sectional area are illustrated in Fig. 2. These kinematic constraints do not include warping (the plane sections remain plane). Besides that, it is considered that w_1, w_2 and w_3 are small when compared to h^e, and $\sin\theta_i \approx \tan\theta_i \approx \theta_i$.

In Euler-Bernoully theory, $\theta_\beta = dw_\gamma/dx$ (plane section remains perpendicular to the neutral axis). On the other hand, in Timoshenko theory $\theta_\beta > dw_\gamma/dx$, as can be observed in Fig. 2.

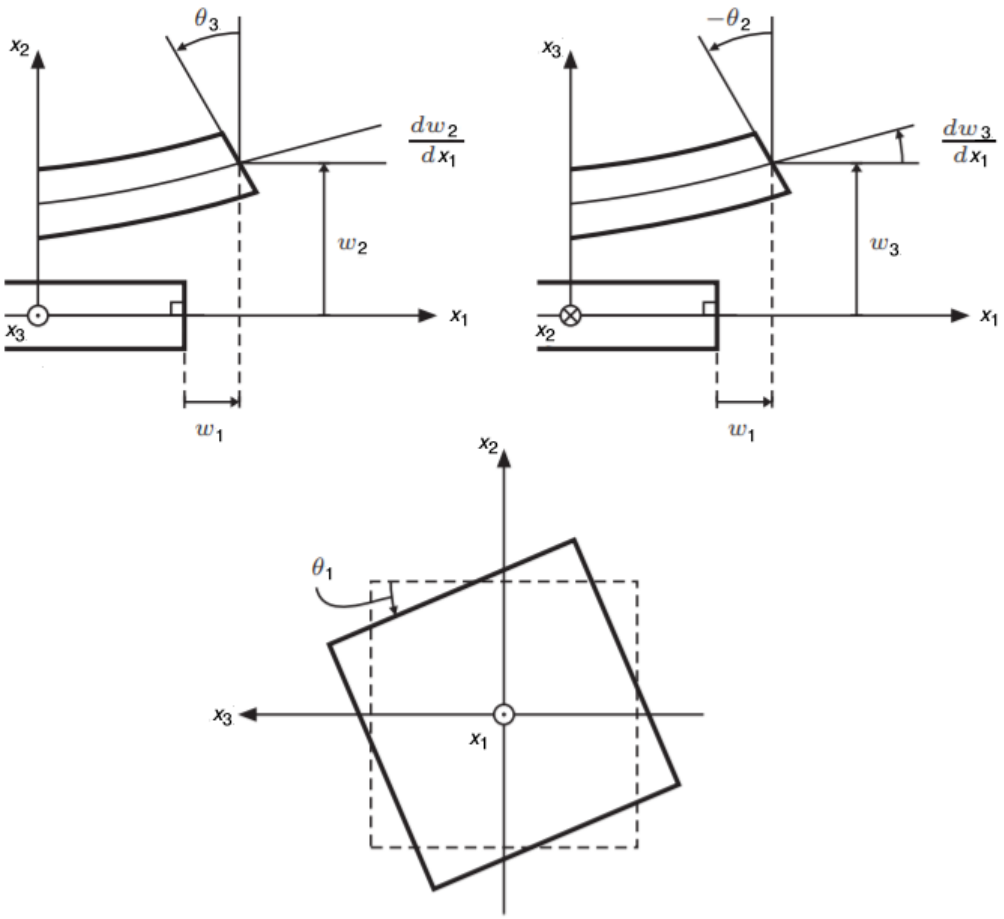

Figure 2: Deformation components in Timoshenko beam theory [1].

3 Mechanical equilibrium and constitutive equation

The local condition of mechanical equilibrium in a continuum medium Ω is given by [3]:

$$\mathbf{div}\boldsymbol{\sigma} + \underline{\mathscr{F}} = \rho\ddot{\boldsymbol{u}}, \tag{9}$$

where the entity $\underline{\mathscr{F}}$ represents the body forces acting on Ω and ρ is the density of the material. Rewriting in Einstein notation (see [3] for a review on index notation):

$$\text{in } \Omega : \begin{cases} \sigma_{ii,i} + \mathscr{F}_i = \rho\ddot{u}_i, \\ \sigma_{ii,i} = C_{ijkl}\epsilon_{kl}, \\ \epsilon_{ij} = u_{(i,j)}; \end{cases} \tag{10}$$

$$\text{on } \Gamma_g : u_i = g_i; \tag{11}$$

and

$$\text{on } \Gamma_k : \sigma_{ii,i}n_j = k_i, \tag{12}$$

where $\mathbf{C}$ is the constitutive tensor, $\boldsymbol{\epsilon}$ is the strain tensor, Γ_g is the boundary of Ω where Dirichlet boundary conditions g_i are applied, and Γ_k is the boundary of Ω where Newmann boundary conditions k_i are applied (at normal direction $\boldsymbol{n}$). The sub-indexes inside parenthesis indicate derivatives. The strain tensor $\boldsymbol{\epsilon}$ and the stress tensor $\boldsymbol{\sigma}$ can be also written in the following vector form:

$$\boldsymbol{\epsilon}(\boldsymbol{u}) = \begin{Bmatrix} u_{(1,1)} \\ u_{(2,2)} \\ u_{(3,3)} \\ u_{(2,3)} + u_{(3,2)} \\ u_{(1,3)} + u_{(3,1)} \\ u_{(1,2)} + u_{(2,1)} \end{Bmatrix}, \tag{13}$$

and

$$\boldsymbol{\sigma}(\boldsymbol{\epsilon}) = \begin{Bmatrix} \sigma_{1,1} \\ \sigma_{2,2} \\ \sigma_{3,3} \\ \sigma_{2,3} \\ \sigma_{1,3} \\ \sigma_{1,2} \end{Bmatrix}. \tag{14}$$

Considering the homogeneous isotropic case [4], we have:

$$\sigma_{ij} = \lambda \epsilon_{kk} \delta_{ij} + 2\mu \epsilon_{ij}, \tag{15}$$

where δ_{ij} is the "delta of Kronecker" (see [3] for a review on continuum mechanics), and λ and μ are the Lamé parameters, which are obtained by:

$$\lambda = \frac{\nu E}{(1+\nu)(1-2\nu)}, \tag{16}$$

and

$$\mu = \frac{E}{2(1+\nu)}. \tag{17}$$

The Young's modulus E and the Poisson's ration ν are intrinsic material properties considering an isotropic media.

Assuming the hypothesis presented in Eq. (4):

$$0 = \sigma_{\beta\gamma} = \lambda \epsilon_{kk} \delta_{\beta\gamma} + 2\mu \epsilon_{\beta\gamma}, \tag{18}$$

which leads to

$$\epsilon_{\beta\beta} = \frac{-\lambda}{\lambda + \mu} \epsilon_{11}, \tag{19}$$

and to

$$\epsilon_{\beta\gamma} = \frac{-\lambda \epsilon_{11}}{2(\lambda + \mu)} \delta_{\beta\gamma}. \tag{20}$$

Using Eqs. (19) and (20) in Eq. (15):

$$\sigma_{11} = \lambda \epsilon_{kk} + 2\mu \epsilon_{11} = \lambda \epsilon_{\beta\beta} + (\lambda + 2\mu) \epsilon_{11}. \tag{21}$$

So,

$$\boxed{\sigma_{11} = E \epsilon_{11}}, \tag{22}$$

and

$$\boxed{\sigma_{\gamma 1} = 2\mu \epsilon_{\gamma 1}}. \tag{23}$$

4 Kinematic relations: strain-displacement equations

Employing the kinematic conditions stated in Section 2.3, we obtain the following relations:

$$\epsilon_{\beta\gamma} = u_{(\beta\gamma)} = 0, \tag{24}$$

$$\epsilon_{11} = w_1' - x_2\theta_3' + x_3\theta_2', \tag{25}$$

$$\epsilon_{21} = \frac{1}{2}(w_2' - x_3\theta_1' - \theta_3), \tag{26}$$

$$\epsilon_{31} = \frac{1}{2}(w_3' + x_2\theta_1' + \theta_2). \tag{27}$$

where the primes denote differentiation with respect to x_1 ($d(\cdot)/dx_1$).

Hughes' remark [4]: As is often the case in beam, the stress and kinematic assumptions lead to "microscopic" inconsistencies. For example, from Section 2.2 we have deduced Eq. (20), whereas we have $\epsilon_{\beta\gamma} = 0$ if calculating as done in Section 4. For purposes of calculating $\sigma_{\beta\gamma 1}$, the former expression is preferred. These inconsistencies ultimately cause no harm, and, as we have remarked previously, the ultimate justification of a "macroscopic" theory such as this one is its usefulness in practical structural engineering applications.

5 Variational equation: principle of virtual work

Consider Eq. (9) the *strong form* of the considered problem. Assuming the virtual displacement field $\overline{\boldsymbol{u}}$ (a kinematic admissible field), the variational equation can be written as [4, 7]:

$$\int_\Omega \overline{u}_{(ij)}\sigma_{ij}d\Omega - \int_\Omega \overline{u}_i\mathscr{F}_i d\Omega - \int_{\Gamma_k} \overline{u}_i k_i d\Gamma + \int_\Omega \overline{u}_i\rho\ddot{u}_i d\Omega = 0. \tag{28}$$

Eq. (28) is obtained from Eq. (9) using the *divergence theorem* (considering a generic function f):

$$\int_\Omega f_{(,i)}d\Omega = \int_\Gamma f n_i d\Gamma, \tag{29}$$

and *integration by parts* (considering generic functions f and g):

$$\int_\Omega f_{(,i)}g d\Omega = -\int_\Omega f g_{(,i)}d\Omega + \int_\Gamma f g n_i d\Gamma. \tag{30}$$

In the next equations, we will adopt (considering $dA = dx_2dx_3$) the following relation:

$$\int_\Omega d\Omega = \sum_{e=1}^{nel}\int_{\Omega_e} d\Omega = \sum_{e=1}^{nel}\int_0^{h_e}\int_{A^e} dA dx_1. \tag{31}$$

Without loss of generality, we shall assume $\Gamma_k = \oslash$ due to the "line shape" of the simplified structure. All distributed external loads (force/length or moment/length) will be considered in the body force vector $\underline{\mathscr{F}}$.

Thus, Eq. (28) can be rewritten as:

$$\begin{aligned} 0 = \sum_{e=1}^{nel}\Bigg\{ &\int_0^{h_e}\int_{A^e}(2\overline{u}_{(\gamma,1)}\sigma_{\gamma 1} + \overline{u}_{(1,1)}\sigma_{11})dA dx_1 \\ &- \int_0^{h_e}\int_{A^e}\overline{u}_i\mathscr{F}_i dA dx_1 + \boxed{\int_0^{h_e}\int_{A^e}\overline{u}_i\rho\ddot{u}_i dA dx_1}\Bigg\}. \end{aligned} \tag{32}$$

Using the properties defined in Eq. (3), Eq. (32) can be written as

$$\begin{aligned}0 =& \sum_{e=1}^{nel}\Bigg\{\int_0^{h_e}\int_{A^e}\Big[(\overline{w}_2' - x_3\overline{\theta}_1' - \overline{\theta}_3)\sigma_{21} + (\overline{w}_3' + x_2\overline{\theta}_1' + \overline{\theta}_2)\sigma_{31} \\ &+ (\overline{w}_1' - x_2\overline{\theta}_3' + x_3\overline{\theta}_2')\sigma_{11}\Big]dAdx_1 - \int_0^{h_e}\int_{A^e}\Big[(\overline{w}_2 - x_3\overline{\theta}_1)\mathscr{F}_2 \\ &+ (\overline{w}_3 + x_2\overline{\theta}_1)\mathscr{F}_3 + (\overline{w}_1 - x_2\overline{\theta}_3 + x_3\overline{\theta}_2)\mathscr{F}_1\Big]dAdx_1 \\ &+ \boxed{\int_0^{h_e}\int_{A^e}\Big[\overline{w}_2\ddot{w}_2 + \overline{w}_3\ddot{w}_3 + \overline{w}_1\ddot{w}_1 + \overline{\theta}_1\ddot{\theta}_1(x_2^2 + x_3^3)} \\ &\boxed{+\overline{\theta}_2\ddot{\theta}_2x_3^2 + \overline{\theta}_3\ddot{\theta}_3x_2^2\Big]\rho dAdx_1}\Bigg\}.\end{aligned} \tag{33}$$

Contracting this relation leads to:

$$\begin{aligned}0 =& \sum_{e=1}^{nel}\Bigg\{\int_0^{h_e}\Big[(\overline{w}_2' - \overline{\theta}_3)q_2 + (\overline{w}_3' + \overline{\theta}_2)q_3 + \overline{w}_1'q_1 + \overline{\theta}_2'm_2 - \overline{\theta}_3'm_3 + \overline{\theta}_1'm_1\Big]dx_1 \\ &- \int_0^{h_e}\Big[\overline{w}_2F_2 + \overline{w}_3F_3 + \overline{w}_1F_1 + \overline{\theta}_2C_2 - \overline{\theta}_3C_3 + \overline{\theta}_1C_1\Big]dx_1 \\ &+ \boxed{\int_0^{h_e}\Big[(\overline{w}_2\ddot{w}_2 + \overline{w}_3\ddot{w}_3 + \overline{w}_1\ddot{w}_1)\rho A^e + \overline{\theta}_1\ddot{\theta}_1\rho J^e + \overline{\theta}_2\ddot{\theta}_2\rho I_2^e + \overline{\theta}_3\ddot{\theta}_3\rho I_3^e\Big]dx_1}\Bigg\},\end{aligned} \tag{34}$$

where

$$I_2^e = \int_{A^e} x_3^2 dA, \tag{35}$$

$$I_3^e = \int_{A^e} x_2^2 dA, \tag{36}$$

$$J^e = \int_{A^e}(x_2^2 + x_3^2)dA = I_2^e + I_3^e, \tag{37}$$

$$q_1 = \int_{A^e}\sigma_{11}dA = E\int_{A^e}(w_1' - x_2\theta_3' + x_3\theta_2')dA = EA^e\epsilon, \tag{38}$$

$$q_2 = \int_{A^e}\sigma_{21}dA = \mu\int_{A^e}(w_2' - x_3\theta_1' - \theta_3)dA = \mu A^e\gamma_2, \tag{39}$$

$$q_2 = \int_{A^e}\sigma_{31}dA = \mu\int_{A^e}(w_3' + x_2\theta_1' + \theta_2)dA = \mu A^e\gamma_3, \tag{40}$$

$$\begin{aligned}m_1 =& \int_{A^e}(\sigma_{31}x_2 - \sigma_{21}x_3)dA = \mu\int_{A^e}\Big[(w_3' + x_2\theta_1' + \theta_2)x_2 \\ &- (w_2' - x_3\theta_1' - \theta_3)x_3\Big]dA = \mu J^e\Psi,\end{aligned} \tag{41}$$

$$m_2 = \int_{A^e}\sigma_{11}x_3dA = E\int_{A^e}(w_1' - x_2\theta_3' + x_3\theta_2')x_3dA = EI_2^e\kappa_2, \tag{42}$$

$$m_3 = \int_{A^e}\sigma_{11}x_2dA = E\int_{A^e}(w_1' - x_2\theta_3' + x_3\theta_2')x_2dA = -EI_3^e\kappa_3. \tag{43}$$

In the equations above: $\kappa_\beta = \theta'_\beta$ is called "curvature"; $\epsilon = w'_1$; $\gamma_2 = w'_2 - \theta_3$; $\gamma_3 = w'_3 + \theta_2$; $F_i = \{F_i^e\}$ and $C_i = \{C_i^e\}$ are the element applied external forces and couples, respectively, per unity length, for $1 \leq e \leq nel$, where

$$F_i^e = \int_{A^e} \mathscr{F}_i dA, \tag{44}$$

$$C_1^e = \int_{A^e} (\mathscr{F}_3 x_2 - \mathscr{F}_2 x_3) dA, \tag{45}$$

$$C_2^e = \int_{A^e} \mathscr{F}_1 x_3 dA, \tag{46}$$

and

$$C_3^e = \int_{A^e} \mathscr{F}_1 x_2 dA. \tag{47}$$

5.1 Weak form of the problem

The variational equation in Eq. (34) is also known as the *weak form* of the problem. The equivalence of strong and weak forms can be proved, as can be seen in [4] and in [2]. However, the weak form enables adopting non smooth trial functions to represent the global displacements, which is the main assumption for implementing the Finite Element Method (FEM).

Rearraging Eq. (34) using Eqs. (35) to (43), we obtain:

$$\begin{aligned} 0 = \sum_{e=1}^{nel} \Bigg\{ & \int_0^{h_e} \Big(\overline{\gamma}_2 \mu A_s^e \gamma_2 + \overline{\gamma}_3 \mu A_s^e \gamma_3 + \overline{\kappa}_2 E I_2^e \kappa_2 + \overline{\kappa}_3 E I_3^e \kappa_3 \\ & + \overline{\epsilon} E A^e \epsilon + \overline{\Psi} \mu J^e \Psi \Big) dx_1 \\ & - \int_0^{h_e} \Big(\overline{w}_2 F_2 + \overline{w}_3 F_3 + \overline{w}_1 F_1 + \overline{\theta}_2 C_2 - \overline{\theta}_3 C_3 + \overline{\theta}_1 C_1 \Big) dx_1 \\ & + \boxed{\int_0^{h_e} \Big((\overline{w}_2 \ddot{w}_2 + \overline{w}_3 \ddot{w}_3 + \overline{w}_1 \ddot{w}_1) \rho A^e + \overline{\theta}_1 \ddot{\theta}_1 \rho J^e + \overline{\theta}_2 \ddot{\theta}_2 \rho I_2^e + \overline{\theta}_3 \ddot{\theta}_3 \rho I_3^e \Big) dx_1} \Bigg\}, \end{aligned} \tag{48}$$

or, using a matricial form (and now emphasizing that the integration is performed over the element length):

$$\begin{aligned} 0 = \sum_{e=1}^{nel} \Bigg\{ & \int_0^{h_e} \Big[\overline{\boldsymbol{\gamma}}^T \mathbf{D}^s \boldsymbol{\gamma} + \overline{\boldsymbol{\kappa}}^T \mathbf{D}^b \boldsymbol{\kappa} + \overline{\epsilon}(EA^e)\epsilon + \overline{\Psi}(\mu J^e)\Psi \Big] dx_1^e \\ & - \int_0^{h_e} \Big[\overline{\boldsymbol{w}}^T \boldsymbol{F} + \overline{\boldsymbol{\theta}}^T \boldsymbol{C} \Big] dx_1^e \\ & + \boxed{\int_0^{h_e} \Big[\overline{\boldsymbol{w}}^T \mathbf{G}^{tr} \ddot{\boldsymbol{w}} + \overline{\boldsymbol{\theta}}^T \mathbf{G}^r \ddot{\boldsymbol{\theta}} \Big] dx_1^e} \Bigg\}, \end{aligned} \tag{49}$$

where

$$\boldsymbol{w} = \begin{Bmatrix} w_1 \\ w_2 \\ w_3 \end{Bmatrix}, \boldsymbol{\theta} = \begin{Bmatrix} \theta_1 \\ \theta_2 \\ \theta_3 \end{Bmatrix}, \tag{50}$$

$$\boldsymbol{\gamma} = \begin{Bmatrix} \gamma_2 \\ \gamma_3 \end{Bmatrix}, \boldsymbol{\kappa} = \begin{Bmatrix} \kappa_2 \\ \kappa_3 \end{Bmatrix}, \tag{51}$$

$$\mathbf{D}^s = \begin{bmatrix} \mu A_s^e & 0 \\ 0 & \mu A_s^e \end{bmatrix}, \mathbf{D}^b = \begin{bmatrix} EI_2^e & 0 \\ 0 & EI_3^e \end{bmatrix}, \tag{52}$$

$$\mathbf{G}^{tr} = \begin{bmatrix} \rho A^e & 0 & 0 \\ 0 & \rho A^e & 0 \\ 0 & 0 & \rho A^e \end{bmatrix}, \tag{53}$$

$$\mathbf{G}^{r} = \begin{bmatrix} \rho J^e & 0 & 0 \\ 0 & \rho I_2^e & 0 \\ 0 & 0 & \rho I_3^e \end{bmatrix}. \tag{54}$$

6 Bubnov-Galerkin method

It is not necessary to assume the same shape functions for transverse and extensional displacements, or for bending and torsional rotations. Arguments can be made, if fact, that there are some conceptual advantages to employing different interpolations in the present context. However, there are practical advantages to employing same shape functions, which can be seen in commercial finite element codes.

We shall assume that [4]:

$$w_i^e(x_1, x_2, x_3, t) = \sum_{a=1}^{npel} \mathrm{N}_a \mathrm{w}_{ia}^e, \tag{55}$$

and

$$\theta_i^e(x_1, x_2, x_3, t) = \sum_{a=1}^{npel} \mathrm{N}_a \theta_{ia}^e, \tag{56}$$

where N_a is the shape function related to the "weights" w_{ia} and θ_{ia} at node a in element e.

In order to obtain the element matrices, we assume the following vector form for the element's degrees of freedom weights and element's load weights:

$$\mathbf{d}^e = \begin{Bmatrix} \mathrm{w}_{11}^e \\ \mathrm{w}_{21}^e \\ \mathrm{w}_{31}^e \\ \theta_{11}^e \\ \theta_{21}^e \\ \theta_{31}^e \\ \vdots \\ \mathrm{w}_{1npel}^e \\ \mathrm{w}_{2npel}^e \\ \mathrm{w}_{3npel}^e \\ \theta_{1npel}^e \\ \theta_{2npel}^e \\ \theta_{3npel}^e \end{Bmatrix}, \tag{57}$$

Consequently,

$$\begin{Bmatrix} w_1^e(x_1,x_2,x_3,t) \\ w_2^e(x_1,x_2,x_3,t) \\ w_3^e(x_1,x_2,x_3,t) \\ \theta_1^e(x_1,x_2,x_3,t) \\ \theta_2^e(x_1,x_2,x_3,t) \\ \theta_3^e(x_1,x_2,x_3,t) \end{Bmatrix} = \mathbf{N}\mathbf{d}^e, \tag{58}$$

where

$$\mathbf{N} = \begin{bmatrix} \mathrm{N}_1 & 0 & 0 & 0 & 0 & 0 & ... & \mathrm{N}_{npel} & 0 & 0 & 0 & 0 & 0 \\ 0 & \mathrm{N}_1 & 0 & 0 & 0 & 0 & ... & 0 & \mathrm{N}_{npel} & 0 & 0 & 0 & 0 \\ 0 & 0 & \mathrm{N}_1 & 0 & 0 & 0 & ... & 0 & 0 & \mathrm{N}_{npel} & 0 & 0 & 0 \\ 0 & 0 & 0 & \mathrm{N}_1 & 0 & 0 & ... & 0 & 0 & 0 & \mathrm{N}_{npel} & 0 & 0 \\ 0 & 0 & 0 & 0 & \mathrm{N}_1 & 0 & ... & 0 & 0 & 0 & 0 & \mathrm{N}_{npel} & 0 \\ 0 & 0 & 0 & 0 & 0 & \mathrm{N}_1 & ... & 0 & 0 & 0 & 0 & 0 & \mathrm{N}_{npel} \end{bmatrix}. \tag{59}$$

Thus there are six degrees of freedom per node, and we can write (from Eq. (49)):

$$\boldsymbol{\kappa} = \mathbf{B}^b\mathbf{d}^e, \tag{60}$$

$$\boldsymbol{\gamma} = \mathbf{B}^s\mathbf{d}^e, \tag{61}$$

$$\boldsymbol{\epsilon} = \mathbf{B}^a\mathbf{d}^e, \tag{62}$$

$$\boldsymbol{\Psi} = \mathbf{B}^t\mathbf{d}^e, \tag{63}$$

$$\boldsymbol{w} = \mathbf{N}^{tr}\mathbf{d}^e, \tag{64}$$

$$\boldsymbol{\theta} = \mathbf{N}^r\mathbf{d}^e, \tag{65}$$

where

$$\mathbf{B}^b = \left[\begin{array}{cccc} \mathbf{B}_1^b, & ..., & \mathbf{B}_{npel}^b \end{array} \right], \tag{66}$$

$$\mathbf{B}^s = \left[\begin{array}{cccc} \mathbf{B}_1^s, & ..., & \mathbf{B}_{npel}^s \end{array} \right], \tag{67}$$

$$\mathbf{B}^a = \left[\begin{array}{cccc} \mathbf{B}_1^a, & ..., & \mathbf{B}_{npel}^a \end{array} \right], \tag{68}$$

$$\mathbf{B}^t = \left[\begin{array}{cccc} \mathbf{B}_1^a, & ..., & \mathbf{B}_{npel}^t \end{array} \right], \tag{69}$$

$$\mathbf{N}^{tr} = \left[\begin{array}{cccc} \mathbf{N}_1^{tr}, & ..., & \mathbf{N}_{npel}^{tr} \end{array} \right], \tag{70}$$

$$\mathbf{N}^r = \left[\begin{array}{cccc} \mathbf{N}_1^r, & ..., & \mathbf{N}_{npel}^r \end{array} \right], \tag{71}$$

$$\mathbf{B}_a^b = \begin{bmatrix} 0 & 0 & 0 & 0 & \mathrm{N}_a' & 0 \\ 0 & 0 & 0 & 0 & 0 & \mathrm{N}_a' \end{bmatrix}, \tag{72}$$

$$\mathbf{B}_a^s = \begin{bmatrix} 0 & \mathrm{N}_a' & 0 & 0 & 0 & -\mathrm{N}_a \\ 0 & 0 & \mathrm{N}_a' & 0 & \mathrm{N}_a & 0 \end{bmatrix}, \tag{73}$$

$$\mathbf{B}_a^a = \begin{bmatrix} \mathrm{N}_a' & 0 & 0 & 0 & 0 & 0 \end{bmatrix}, \tag{74}$$

$$\mathbf{B}_a^t = \begin{bmatrix} 0 & 0 & 0 & \mathrm{N}_a' & 0 & 0 \end{bmatrix}, \tag{75}$$

$$\mathbf{N}_a^{tr} = \begin{bmatrix} \mathrm{N}_a & 0 & 0 & 0 & 0 & 0 \\ 0 & \mathrm{N}_a & 0 & 0 & 0 & 0 \\ 0 & 0 & \mathrm{N}_a & 0 & 0 & 0 \end{bmatrix}, \tag{76}$$

$$\mathbf{N}_a^r = \begin{bmatrix} 0 & 0 & 0 & \mathrm{N}_a & 0 & 0 \\ 0 & 0 & 0 & 0 & \mathrm{N}_a & 0 \\ 0 & 0 & 0 & 0 & 0 & \mathrm{N}_a \end{bmatrix}, \tag{77}$$

with $1 \leq a \leq npel$.

With these definitions, we obtain the following expressions for the stiffness, mass and load (with respect to the local coordinate system):

$$\boxed{\mathbf{K}^e = \mathbf{K}_b^e + \mathbf{K}_s^e + \mathbf{K}_a^e + \mathbf{K}_t^e}, \tag{78}$$

$$\mathbf{K}_b^e = \int_0^{h_e} \mathbf{B}^{bT} \mathbf{D}^b \mathbf{B}^b dx_1^e, \text{ (bending stiffness)} \tag{79}$$

$$\mathbf{K}_s^e = \int_0^{h_e} \mathbf{B}^{sT} \mathbf{D}^s \mathbf{B}^s dx_1^e, \text{ (shear stiffness)} \tag{80}$$

$$\mathbf{K}_a^e = \int_0^{h_e} \mathbf{B}^{aT} (EA) \mathbf{B}^a dx_1^e, \text{ (axial stiffness)} \tag{81}$$

$$\mathbf{K}_t^e = \int_0^{h_e} \mathbf{B}^{tT} (\mu J) \mathbf{B}^t dx_1^e, \text{ (torsional stiffness)} \tag{82}$$

$$\boxed{\mathbf{M}^e = \mathbf{M}_{tr}^e + \mathbf{K}_r^e}, \tag{83}$$

$$\mathbf{M}_{tr}^e = \int_0^{h_e} \mathbf{N}^{trT} \mathbf{G}^{tr} \mathbf{N}^{tr} dx_1^e, \text{ (translational mass)} \tag{84}$$

$$\mathbf{M}_r^e = \int_0^{h_e} \mathbf{N}^{rT} \mathbf{G}^r \mathbf{N}^r dx_1^e, \text{ (rotational mass)} \tag{85}$$

and

$$\mathbf{p}^e = \int_0^{h_e} \mathbf{N}^T \begin{Bmatrix} F_1 \\ F_2 \\ F_3 \\ C_1 \\ C_2 \\ C_3 \end{Bmatrix} dx_1^e. \tag{86}$$

7 Element coordinates and shape functions

The equations above was obtained considering operations in the global coordinate system. However, one of the advantages of FEM is to carry out mathematical operations in the local coordinate system of each element. In this work, the element coordinate system adopted is illustrated at the bottom of Fig. 3.

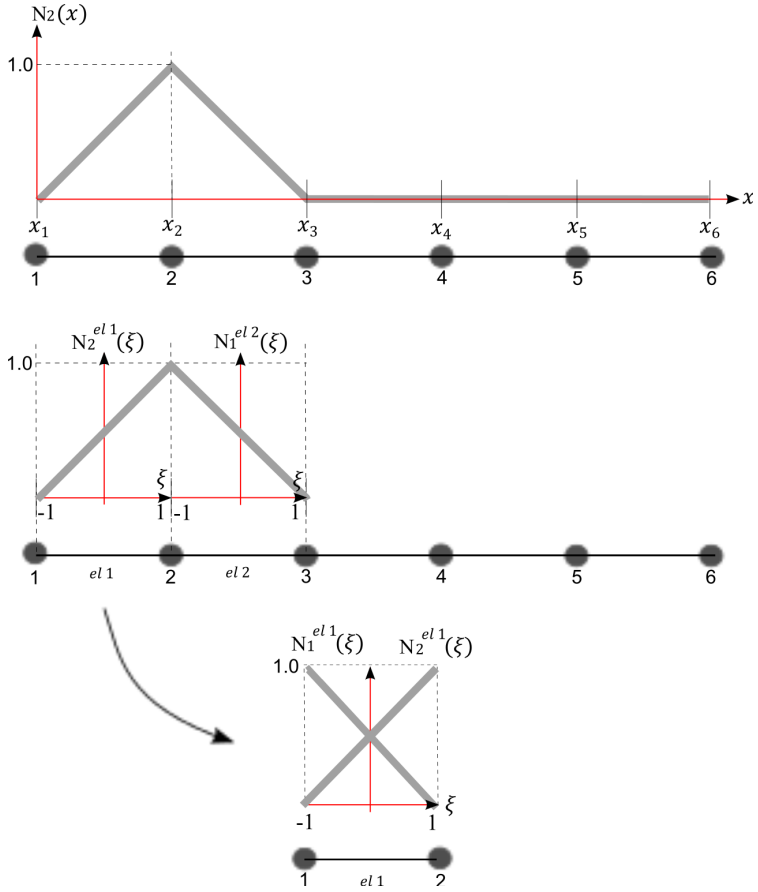

Figure 3: Element coordinates [Source: author].

The mapping from global to element coordinates is performed as in Eqs. 57 and 58. In *OpenPulse* we consider the following linear shape functions:

$$N_1(\xi) = \frac{1}{2}(1-\xi), \qquad N_2(\xi) = \frac{1}{2}(1+\xi). \tag{87}$$

With the change of variables, the differential dx_1 in the necessary integrations is replaced by

$$dx_1 = det\mathbf{J}d\xi, \tag{88}$$

where, for this specific case [7],

$$det\mathbf{J} = \frac{\partial x_1}{\partial \xi} = \frac{1}{2}l_e. \tag{89}$$

IMPORTANT NOTE: $\mathbf{B}(x) = \mathbf{J}^{-1}\mathbf{B}(\xi)$.

8 Numerical integration

OpenPulse employs Gauss quadrature to evaluate the integrals in the weak formulation over a symmetrical range of ξ from -1 to 1.

It uses one point of integration along the length for element stiffness matrix (in order to avoid locking effects), and two points for element mass matrix.

- Stiffness: $\xi_1 = 0$; $\text{weight}_1 = 2$;
- Mass: $\xi_1 = -\sqrt{3}/3$; $\xi_2 = \sqrt{3}/3$; $\text{weight}_1 = 1$; $\text{weight}_2 = 1$.

9 Element transformation matrix

In Sections 6 and 7, the element stiffness and mass matrices are obtained considering a local coordinate system parallel to the reference coordinate system. However, 3D pipe systems require a transformation of each element into the its real position. The element transformation matrix **TR** is defined as:

$$\mathbf{TR} = \begin{bmatrix} \mathbf{T} & 0 & 0 & 0 \\ 0 & \mathbf{T} & 0 & 0 \\ 0 & 0 & \mathbf{T} & 0 \\ 0 & 0 & 0 & \mathbf{T} \end{bmatrix}, \tag{90}$$

where

$$\mathbf{T} = \begin{bmatrix} C_1C_2 & S_1C_2 & S_2 \\ -C_1S_2S_3 - S_1C_3 & -S_1S_2S_3 + C_1C_3 & S_3C_2 \\ -C_1S_2C_3 + S_1S_3 & -S_1S_2C_3 - C_1S_3 & C_3C_2 \end{bmatrix}, \tag{91}$$

with

$$S_1 = (y_2 - y_1)/l_{xy} \quad \text{if} \quad l_{xy} < d_l; \tag{92}$$
$$S_1 = 0 \quad \text{if} \quad l_{xy} \leq d_l; \tag{93}$$
$$S_2 = (z_2 - z_1)/l_e; \tag{94}$$
$$S_3 = \sin\theta_l; \tag{95}$$
$$C_1 = (x_2 - x_1)/l_{xy} \quad \text{if} \quad l_{xy} < d_l; \tag{96}$$
$$C_1 = 1 \quad \text{if} \quad l_{xy} \leq d_l; \tag{97}$$
$$C_2 = l_{xy}/l_e; \tag{98}$$
$$C_3 = \cos\theta_l. \tag{99}$$

In the equations above, l_e is the element length, $l_{xy} = \sqrt{(x_2 - x_1)^2 + (y_2 - y_1)^2}$; $d = 0.0001 l_e$ and $\theta_l = 0$. Indexes 1 and 2 for coordinates x, y and z refer to the node position considering the respective element connectivity.

10 Matrix assembly

Noting that the global vector $\mathbf{d}$ is obtained by $\mathbf{d} = \biguplus_{e=1}^{nel} \mathbf{d}^e$ (assembly process, considering elements that share same degrees of freedom), we can rewrite Eq. (49) as:

$$\overline{\mathbf{d}}^T \left[\biguplus_{e=1}^{nel} \mathbf{K}^e \right] \mathbf{d} + \overline{\mathbf{d}}^T \left[\biguplus_{e=1}^{nel} \mathbf{M}^e \right] \ddot{\mathbf{d}} = \overline{\mathbf{d}}^T \left\{ \biguplus_{e=1}^{nel} \mathbf{p}^e \right\}. \tag{100}$$

So, the global matrices and load vector are defined as:

$$\mathbf{K} = \left[\bigcup_{e=1}^{nel} \mathbf{K}^e \right]; \mathbf{M} = \left[\bigcup_{e=1}^{nel} \mathbf{M}^e \right]; \mathbf{p} = \left\{ \bigcup_{e=1}^{nel} \mathbf{p}^e \right\}. \tag{101}$$

And, considering any (but admissible) $\overline{\boldsymbol{d}}$:

$$\mathbf{K}\mathbf{d} + \mathbf{M}\ddot{\mathbf{d}} = \mathbf{p}. \tag{102}$$

For numerical implementation in Python, see Theory Reference C.

11 Damping model

The damping matrix $\mathbf{C}$ used in harmonic analysis (considering only the material damping) is defined as

$$\mathbf{C} = \alpha\mathbf{M} + (\beta + \frac{1}{\omega}\eta)\mathbf{K}, \tag{103}$$

where α is the mass-proportional coefficient, β is stiffness-proportional coefficient, and η is the structural (hysteretic) damping. $\omega = 2\pi f$, where f is the excitation frequency.

12 Shear correction factor

In OpenPulse, the shear correction factor μ used in the calculation of $\mathbf{K}_s^e$ was adapted from Pilkey's book [6] (more details will be presented in V2.0 of this Theory Reference). It is performed a numerical integration over the cross-section to obtain the section's constants and the shear correction factors. The cross-sectional area is composed of N elements (default for calculations: N=64). However, the simplified equation found in [5] is a very good approximation for thin and thick walled pipes:

$$\mu = \frac{6}{(7 + 20k^2)}, \tag{104}$$

where

$$k = \frac{a}{1 + a^2}, \tag{105}$$

and $a = d_i/d_o$, with d_i and d_o being external and internal diameter of the pipe section, respectively.

13 Prescribed forces and moments

See Eq. 86 for distributed forces and moments. For nodal forces and moments, the value can be inserted directly in the respective entry of $\mathbf{p}$ in Eq. 102.

14 Themes to be presented in Theory Reference D (which depend on the Analysis Types)

- prescribed displacements;
- internal pressure loads;

- springs, masses and dampers;
- Stress calculation in vibration problems.

References

[1] L. Andersen and S. R. K. Nielsen. *Elastic Beams in Three Dimensions*. DCE Lecture Notes No. 23 - Aalborg University, 2008.

[2] J. Fish and T. Belytschko. *A First Course in Finite Elements*. Wiley, 2007.

[3] G. A. Holzapfel. *Nonlinear Solid Mechanics: A Continuum Approach for Engineering*. Wiley, 2000.

[4] T. J. R. Hughes. *The Finite Element Method: Linear Static and Dynamic Finite Element Analysis*. Dover, 2000.

[5] E. Oñate. *Structural Analysis with the Finite Element Method. Linear Statics. Volume 2: Beams, Plates and Shells*. CIMNE, 2013.

[6] W. D. Pilkey. *Anslysis and Desing of Elastic Beams: Computational Methods*. John Wiley & Sons, Inc., 2002.

[7] O. C. Zienkiewicz and R. L. Taylor. *The Finite Element Method For Solid and Structural Mechanics*. Butterworth-Heinemann, 2005.